Stabilization of Octahedral Metal Halide Clusters by Host–Guest Complexation with γ-Cyclodextrin: Toward Nontoxic Luminescent Compounds

Anton Ivanov, Mohamed Haouas, Darya Evtushok, Tatiana Pozmogova, Tatiana Golubeva, Yann Molard, Stéphane Cordier, Clément Falaise, Emmanuel Cadot, Michael Shestopalov

Stabilization of Octahedral Metal Halide Clusters by Host-Guest Complexation with γ-Cyclodextrin: Toward Non-Toxic Luminescent Compounds

Anton A. Ivanov,[†,‡] Mohamed Haouas,*[†] Darya V. Evtushok,[‡] Tatiana N. Pozmogova,[‡] Tatiana S. Golubeva,[§,‖] Yann Molard,[▽] Stéphane Cordier,[▽] Clément Falaise,[†] Emmanuel Cadot,[†] and Michael A. Shestopalov*[‡]*

[†]Institut Lavoisier de Versailles, UMR 8180 CNRS, UVSQ, Université Paris-Saclay, Versailles, France. E-mail : mohamed.haouas@uvsq.fr

[‡]Nikolaev Institute of Inorganic Chemistry SB RAS, Novosibirsk, 630090, Russia. E-mail: ivanov338@niic.nsc.ru, shtopy@niic.nsc.ru

[§]Novosibirsk State University, Novosibirsk, Russia.

[‖]Federal Research Center Institute of Cytology and Genetics SB RAS, Novosibirsk, Russia.

[▽]Université de Rennes, CNRS, ISCR - UMR 6226, ScanMAT – UMS 2001, F-35000 Rennes.

KEYWORDS. Molybdenum, tungsten, metal clusters, cyclodextrin, NMR, stability, luminescence, cell penetration, cytotoxicity.

ABSTRACT. γ-cyclodextrin (γ-CD) interacts in aqueous solution with octahedral halide clusters $Na_2[\{M_6X_8\}Cl_6]$ (M = Mo, W; X = Br, I) to form robust inclusion supramolecular complexes $[\{M_6X_8\}Cl_6@2\gamma\text{-CD}]^{2-}$. Single crystal X-ray diffraction analyses revealed two conformational organizations within the adduct depending on the nature of the inner halide X within the $\{M_6X_8\}$ core. Using ^{35}Cl NMR and UV-vis as complementary techniques, the kinetics of the hydrolysis process were shown to increase with the following order: $\{W_6I_8\} < \{W_6Br_8\} \approx \{Mo_6I_8\} < \{Mo_6Br_8\}$. The complexation with γ-CD enhances drastically the hydrolytic stability of luminescent $[\{M_6X_8\}Cl_6]^{2-}$ cluster-based units, which was quantitatively proved by the same techniques. The resulting host-guest complexation provides a protective shell against contact with water and offers promising horizons for octahedral clusters in biology as revealed by the low dark cytotoxicity and cellular uptake.

INTRODUCTION

Native cyclodextrins (CDs) are cheap drug carriers widely used in pharmacology.[1] Recent reports demonstrated that γ-CD, an macrocyclic oligosaccharide built on eight glucopyranose units defining a cavity of 10 Å (Figure 1), can host various types of inorganic polynuclear species,[2-6] and even stabilize hydrolytically fragile polyoxometalates and Fe-S clusters in water.[7-10] The chaotropic effect has been identified as the main contributor of such supramolecular associations, where water solvation plays prominent role in stabilizing these types of hybrid complexation.[11, 12] $[\{M_6X_8\}L_6]^n$ octahedral-cluster based units represent multifunctional nano-sized building blocks composed of a robust $\{M_6X_8\}^{4+}$ cluster core (M = Mo or W and X = halides) decorated by six interchangeable apical ligands (L) such as halides, H_2O, or organic ligands (Figure 1). These clusters exhibit both bright phosphorescence in the therapeutic window upon photo- or X-ray

irradiation and ability to photoinduce singlet oxygen production.[13-15] The photo-physical features of $[\{M_6Br_8\}Cl_6]^{2-}$ and $[\{M_6I_8\}Cl_6]^{2-}$ cluster-based units make them particularly appealing for biological applications.[16-19] Nevertheless, the low stability of the octahedral halide molybdenum or tungsten cluster complexes in aqueous media is a serious obstacle to their use in biomedicine. This weak stability in water is a consequence of the fast exchange of apical ligands with water or hydroxo groups, resulting in their precipitation.

We recently reported the preparation of supramolecular adducts between Mo-based clusters and γ-CD leading to a strong sandwich type complexation in the solid-state of general formula $Na_2[\{Mo_6X_8\}Cl_6@2\gamma\text{-CD}]$, where X = Br or I.[20] Herein, we evidence the encapsulation of $[\{M_6X_8\}Cl_6]^{2-}$ units (M = Mo, W; X = Cl, Br, I) within γ-cyclodextrin (Figure 1) cavity slowing down dramatically the hydrolysis processes of the cluster as supported by kinetic studies using ^{35}Cl NMR and UV-vis techniques. Then, we evaluate the biological potentialities of the supramolecular host-guest complexes $[\{M_6X_8\}Cl_6@2\gamma\text{-CD}]^{2-}$ (Figure 2) by studying their cytotoxicity and their cellular uptake on both cancer and normal cell lines.

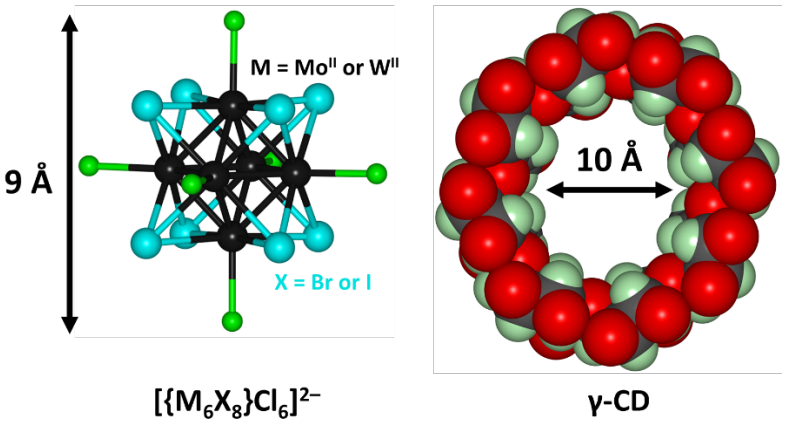

Figure 1. Illustrations showing the molecular entities involved in this study: the octahedral halide clusters $[\{M_6X_8\}Cl_6]^{2-}$ (left) and the γ-cyclodextrin (right). Color code: M – black, X – cyan, Cl – green, C – grey, H – light green.

EXPERIMENTAL SECTION

Syntheses

The compounds $Na_2[\{Mo_6Br_8\}Cl_6]\cdot Me_2CO$ (**MoBr**), $Na_2[\{Mo_6Br_8\}Cl_6]\cdot 2Me_2CO$ (**MoI**), $Na_2[\{W_6Br_8\}Cl_6]\cdot 2Me_2CO$ **(WBr),** $Na_2[\{W_6I_8\}Cl_6]\cdot Me_2CO$ **(WI),** $Na_2[\{Mo_6Br_8\}Cl_6@2\gamma\text{-CD}]\cdot 15H_2O$ **(MoBr@CD),** $Na_2[\{Mo_6Br_8\}Cl_6@2\gamma\text{-CD}]\cdot(\gamma\text{-CD})\cdot 45H_2O$ **(MoBr@CD·CD),** $Na_2[\{Mo_6I_8\}Cl_6@2\gamma\text{-CD}]\cdot 11H_2O$ **(MoI@CD),** $Na_2[\{Mo_6I_8\}Cl_6@2\gamma\text{-CD}]\cdot(\gamma\text{-CD})\cdot 45H_2O$ **(MoI@CD·CD),** $Na_2[\{W_6Br_8\}Cl_6@2\gamma\text{-CD}]\cdot 9H_2O$ **(WBr@CD),** $Na_2[\{W_6Br_8\}Cl_6@2\gamma\text{-CD}]\cdot(\gamma\text{-CD})\cdot 15H_2O$ **(WBr@CD·CD)**, $Na_2[\{W_6I_8\}Cl_6@2\gamma\text{-CD}]\cdot 13H_2O$ **(WI@CD)**, and $Na_2[\{W_6I_8\}Cl_6@2\gamma\text{-CD}]\cdot(\gamma\text{-CD})\cdot 16H_2O$ **(WI@CD·CD)** were synthesized as described in literature.[20,21]

Physical methods

Fourier Transform Infrared (FTIR) spectra (Figures S48-S49) were recorded on a 6700 FT-IR Nicolet spectrophotometer in the range 400-4000 cm^{-1}. Thermogravimetric analysis (TGA) was performed on Mettler Toledo TGA/DSC 1, STARe System apparatus under oxygen flow (50 $mL.min^{-1}$) at a heating rate of 5 °C·min^{-1} up to 700 °C. Energy-dispersive X-ray Spectroscopy (EDS) measurements were performed using a SEM-FEG (Scanning Electron Microscope enhanced by a Field Emission Gun) equipment (JSM 7001-F, Jeol). Elemental CHNS analysis was performed on a EuroVector EA3000 CHNS analyzer.

Single-crystal X-Ray Diffraction analysis (XRD)

Crystals of titled compounds were selected under polarizing optical microscope and glued in paratone oil to prevent any loss of crystallization water. X-ray intensity data were collected at low temperature on a Bruker D8 VENTURE diffractometer equipped with a PHOTON 100 CMOS bidimensional detector using a high brilliance IμS microfocus X-ray Mo K_α monochromatized radiation ($\lambda = 0.71073$ Å). Data reduction was accomplished using SAINT V7.53a. The substantial redundancy in data allowed a semi-empirical absorption correction (SADABS V2.10) to be applied, on the basis of multiple measurements of equivalent reflections. Using Olex2,[22] the structure was solved with the ShelXT[23] structure solution program using Intrinsic Phasing and refined with the ShelXL[24] refinement package using Least Squares minimization. The remaining non-hydrogen atoms were located from Fourier differences and were refined with anisotropic thermal parameters. Positions of the hydrogen atoms belonging to the cyclodextrins were calculated. Crystallographic data for single-crystal X-ray diffraction studies are summarized in Table S1 in the Supporting Information, while CCDC 2097961-2097964 contain the supplementary crystallographic data for this paper. These data can be obtained free of charge from the Cambridge Crystallographic Data Centre via www.ccdc.cam.ac.uk/data_request/cif.

Nuclear magnetic resonance spectroscopy (NMR)

All NMR spectra were measured at 27 °C on a Bruker Avance 400 spectrometer. ^{35}Cl and ^{1}H NMR spectra were measured at Larmor frequencies of 39.2 and 400.1 MHz, respectively. Chemical shifts were referenced to 2 M KCl aqueous solution and TMS, respectively. Measurements were recorded in quantitative mode for kinetics studies. 5 mm NMR tube is used in which is filled with 600 μL D_2O solution of known amount of sample. ^{1}H NMR spectra were recorded accumulating 8 scans, and using 3 s acquisition time, 1 s relaxation delay, and 2.8 μs π/6-pulse width. ^{35}Cl spectra were collected with ca. 2000 number of scans, 200 ms acquisition time, 100 ms relaxation delay, and 21 μs π/2-pulse width. Total measurement time was ca. 10 min. Signal intensity is measured by simulation using NMR Notebook software, and signal area is calibrated using 1-4 mM NaCl solutions as external references to convert into number of moles of Cl^- (see Figure S4 in the Supporting Information). Data were analysed with first-order kinetics model using OriginPro2015 software.

Electronic absorption spectrophotometry

UV-vis spectra were recorded for solutions of compounds in water or acetone on a spectrometer Perkin-Elmer Lambda-750 and Ultrospec 3300 pro. The compounds were dissolved in water to have a C = 2mM. To measure UV-vis spectra the solutions were diluted 100 times. Before each measurement, the solutions were filtered through a syringe filter to remove any precipitate.

Luminescent measurements

The absolute quantum yields were measured using a C9920–03 Hamamatsu system equipped with a 150 W xenon lamp, a monochromator, an integrating sphere and a red-NIR sensitive PMA-

12 detector. Lifetime measurements and TRPL mapping were performed using a picosecond laser diode (Jobin Yvon deltadiode, 375 nm) and a Hamamatsu C10910-25 streak camera mounted with a slow single sweep unit. Signals were integrated on a 30 nm bandwidth. Fits were obtained using ORIGIN software and the goodness of fit was judged by the reduced χ^2 value and residual plot shape. Steady state O_2 ($^1\Delta_g$) measurements were realised with a Hamamatsu H12397-75 NIR-PMT unit mounted on an IHR3 spectrometer. Excitation of samples was realised with a 375 nm laser pulsed diode (Jobin Yvon deltadiode). The system was also equipped with a TCSPC unit to measure the emission lifetime. The luminescence spectra were smoothed by the Savitzky–Golay filter to increase the signal-to-noise ratio.[25]

Cell cultures

HeLa cancer cell line (cervical carcinoma) was obtained from the ATCC (ATCC number CCL-2). The human fibroblasts NAF2nor cell line was kindly provided by a Collective Center of ICG SB RAS Collection of Pluripotent Human and Mammalian Cell Cultures for Biological and Biomedical Research. The cells were maintained in DMEM plus 10% FBS (Gibco), under 37 °C, atmosphere of 5% of CO_2 and 90% humidity.

MTT assay

The effect of **MX@CD** on the cells metabolic activity was determined using the 3-[4,5-dimethylthiazol-2-yl]-2,5-diphenyltetrazolium bromide (MTT) colorimetric assay. HeLa and NAF2nor cells were seeded into 96-well plates at 7×10^3 cells/well and incubated in a medium containing **MX@CD** with concentrations from 2 to 1250 μM for 72 h under 5% CO^2 atmosphere. After the incubation period, 10 μL of the MTT solution (5 mg·mL^{-1}) was added to each well, and the plates were incubated for a further 4 h. Then, the MTT-containing medium was removed and

the formazan crystals were dissolved in 100 μl of DMSO. Absorbance was measured at 492 nm using a microplate reader Mindray MR-96A (Mindray, China). The cell viability percentage was calculated using the following formula: Viability (%) = OD (treated cells)/OD (untreated cells) × 100, where OD was an optical density of solution.

Confocal microscopy

HeLa and NAF2nor cells were planted on an ibidi μ-Slide 8 Well at a density of 5×10^3 cells/well and incubated for 24 hours. After that, **MX@CD** in concentration 156 μM were added to the cells. After incubation for 24 hours, cells were stained with Hoechst 33342 (Thermo Fisher scientific) for 10 minutes under standard cultivation conditions. Microscopic examination was carried out on LSM 510 META (Carl Zeiss) confocal scanning microscope at the Center for Microscopic Analysis of Biological Objects of the Institute of Cytology and Genetics SB RAS. Standard filters were used for clusters (408 nm for excitation and 650 nm for emission). The results were processed using Zen (Carl Zeiss) software.

Flow cytometry

For flow cytometry analysis cells were seeded with a density of 10^5 cells/well in a 6-well plate. The cells were incubated for 24 h, and then washed with PBS. After that, to each well the solutions of studied compounds were added. After 24 h of incubation cells were harvested with trypsin (Capricorn), washed with PBS twice and immediately analyzed on a CytoFLEX cytofluorimeter. The compounds were analysed in PE-Cy7 channel (Excitation 488 and 532 nm; Emission 785 nm).

Photoinduced cytotoxicity study

The HeLa and IHF cells were seeded in 96-well plates at a density of 7×10^3 cells/well and cultured for 24 h. The medium was then replaced with a fresh medium containing **MX@CD** in concentration of 31.25–125 μM and incubated for 24 h. Cells were then illuminated with 500 W halogen lamp ($\lambda \geq 400$ nm) for 30 min. The cells cultured in the free medium were used as a control. Cell viability was assayed after irradiation using MTT-assay. 10 μL of the MTT solution (5 $mg.mL^{-1}$) was added to each well, and the plates were then incubated for 4 h. The resultant formazan was then dissolved in DMSO (100 μL). The optical density was measured with a plate reader Mindray MR-96A (Mindray, China) at a wavelength of 492 nm.

Results and discussion

Isolation, crystal structure and study in solution of supramolecular adducts $Na_2[\{M_6X_8\}Cl_6@2\gamma\text{-CD}]$

The presence of γ-CD in an aqueous solution of $Na_2[\{M_6X_8\}Cl_6]$ (M = Mo, W; X = Cl, Br, I) prevents hydrolysis and precipitation of all studied compounds for at least several days. Using the simple previously published approach,[20] namely crystallization upon slow evaporation of an aqueous solution containing cluster and γ-CD in ratio of 2:1 and 3:1 (for W-clusters only), crystalline products of both previously described molybdenum clusters (noted **MoBr@CD** and **MoI@CD**) and new inclusion compounds based on tungsten clusters (noted **WBr@CD**, **WI@CD**, **WBr@CD·CD** and **WI@CD·CD**, see Experimental part) were obtained. The composition of the compounds was confirmed by elemental analysis, and the crystal structure of the three new compounds was studied by the single-crystal X-ray diffraction analysis, revealing sandwich-type supramolecular complexes.

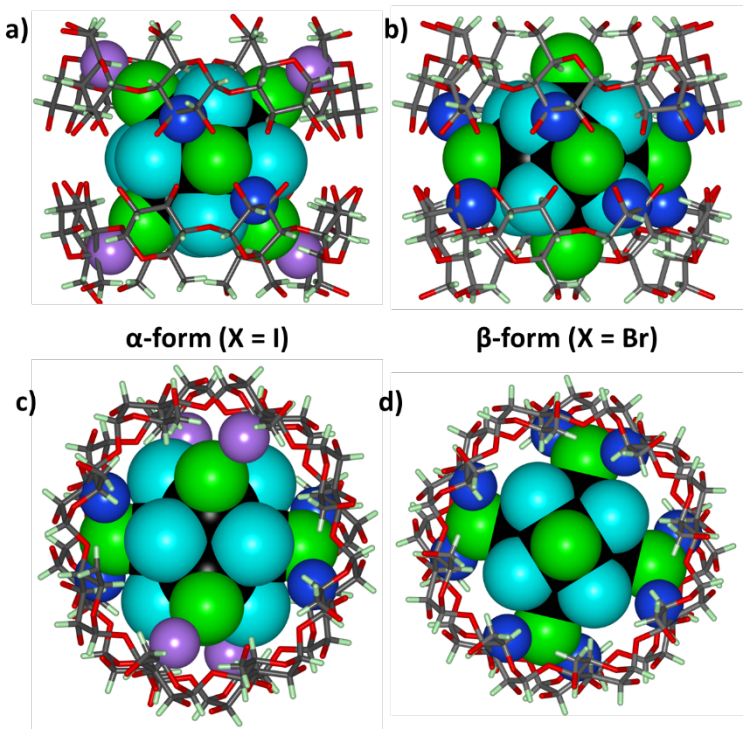

Figure 2. Illustrations of the two types of 2:1 host-guest assembly observed in $[\{M_6X_8\}Cl_6@2\gamma\text{-CD}]^{2-}$ compounds (α-type for X = I and β-type for X = Br): side (a and b) and top views (c and d). The representations of supramolecular adducts shown correspond to crystallographic structures for $[\{W_6Br_8\}Cl_6@2\gamma\text{-CD}]^{2-}$ and $[\{W_6I_8\}Cl_6@2\gamma\text{-CD}]^{2-}$ which are isostructural to Mo-derivatives.[20] Color code: M – black, X – cyan, Cl – green, C – grey, H – light green, H3 and H5 involved in hydrogen bonds – blue and violet spheres respectively.

As in the case of molybdenum clusters, the main structural motif of the tungsten compounds consist of an inclusion complex of cluster anion $[\{W_6X_8\}Cl_6]^{2-}$ embedded into two γ-CDs, interacting with their secondary rims (Figure 2), while compounds **WBr@CD·CD** and **WI@CD·CD** contain additionally co-crystallized γ-CD molecule. Moreover, the cluster inside CDs could adopt two different orientations, leading to two different types of 2:1 inclusion complexes, that we called α and β to differentiate them (see Figure 2a and 2b). In case of

WBr@CD·CD, adopting β-form, cluster's four chlorine ligands are positioned in equatorial plane *a*, parallel to the secondary face of the CD, forming eight relatively strong Cl···H3-C hydrogen bonds (see Figure 3 for numbering of protons). From such an arrangement, two apical chlorine ligands are exposed to the exterior of the host-guest complex. Short contacts between chloride atoms and the inner protons of CD are also pinpointed. On the other hand, in **WI@CD** and **WI@CD·CD** adopting α-form, the complex is rotated 45 degrees (see Figure 2a and c), so that the all chlorine ligands are located inside the cavities of the CDs, restructuring hydrogen bonds to four Cl···H3-C and four Cl···H5-C contacts. The packing of the inclusion compounds occurs through primary faces of the CDs in **WI@CD** and by the co-crystallized empty CD for **WX@CD·CD**, to form tubular "bamboo-like" structures $-\{CD@M_6@CD\}_n-$ and $-\{CD–CD@M_6@CD–CD@M_6@CD\text{-}CD\}_n-$ correspondingly (see Figure S1, in the Supporting Information). Sodium cations and solvate water molecules contribute to the 3D organization of the systems and are located in the cavities between the tubules.

The interaction in aqueous solution between the cluster compounds and the γ-CD was monitored by ^{1}H NMR (Figure 3, Figures S2-S3 in the Supporting Information). As already observed in previous study with the Mo derivatives,[20] there is a clear difference in the host–guest behavior in solution depending on the nature of the conformation in the adduct (α-form *vs* β-form). Indeed, the ^{1}H NMR signals of CD in the presence of the bromide cluster $[W_6Br_8Cl_6]^{2-}$ reveal a strong shift of H3, corresponding to the fingerprint of the β-form arrangement. On the other hand, the inclusion complex built from the iodide cluster $[W_6I_8Cl_6]^{2-}$ which favors the α-form arrangement is characterized by ^{1}H NMR shifts and broadening of both H3 and H5 signals. The NMR spectra of the iodine derivative are broader than those obtained with Br-based clusters (see Figures S2-S3). Consistently with XRD analysis, the ^{1}H NMR titration experiments evidence 2:1 host–guest

systems typical for dynamically frozen complexes usually observed with octahedral metal clusters.[2-4] Such a behavior originates from a complexation driven by the chaotropic effect where the desolvation of guest and association to neutral surfaces like the hydrophobic CD cavities are highly favorable processes.[3, 11, 12] Thus, we can conclude that there is no apparent significant effect of the metal in cluster core both on the formation of crystal structures and on the interaction in aqueous solution, while the inner halogen-ligand plays a key role. This observation indicates the supramolecular recognition is quite sensitive to the cluster size (the volume of cluster $[\{M_6X_8\}Cl_6]^{2-}$ is about 395 and 447 Å^3 for X = Br and I, respectively).

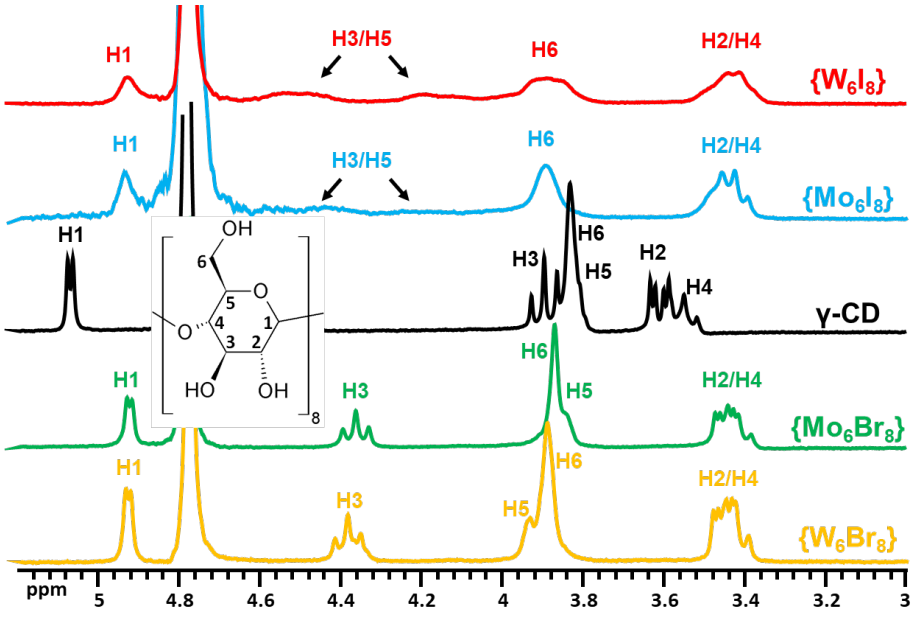

Figure 3. ^{1}H NMR spectra of 2 mM γ-CD in D_2O before (middle), and after addition of 0.5 equivalent of bromide (bottom) and iodide (top) clusters $Na_2[\{M_6X_8\}Cl_6]$.

Stability of clusters $[\{M_6X_8\}Cl_6]^{2-}$ and stabilization effect of γ-CD in aqueous solution

Molybdenum and tungsten chloride clusters are known to be hydrolytically instable. After dissolution of the sodium salt of cluster units (C = 2 mM), the aqueous solutions became quickly

turbid. The EDX analysis of the yellow/orange solids recovered by centrifugation is consistent with the neutral aqua-complex $[\{M_6X_8\}(H_2O)_2Cl_4]$ as proposed by previous reports describing hydrolysis in mineral acids.[26, 27] The formation of insoluble solid is the consequence of stepwise hydrolysis reactions according to equations 1 and 2.

$$[\{M_6X_8\}Cl_6]^{2-} + H_2O \rightarrow [\{M_6X_8\}(H_2O)Cl_5]^{-} + Cl^{-} \quad (1)$$

$$[\{M_6X_8\}(H_2O)Cl_5]^{-} + H_2O \rightarrow [\{M_6X_8\}(H_2O)_2Cl_4]_{\downarrow} + Cl^{-} \quad (2)$$

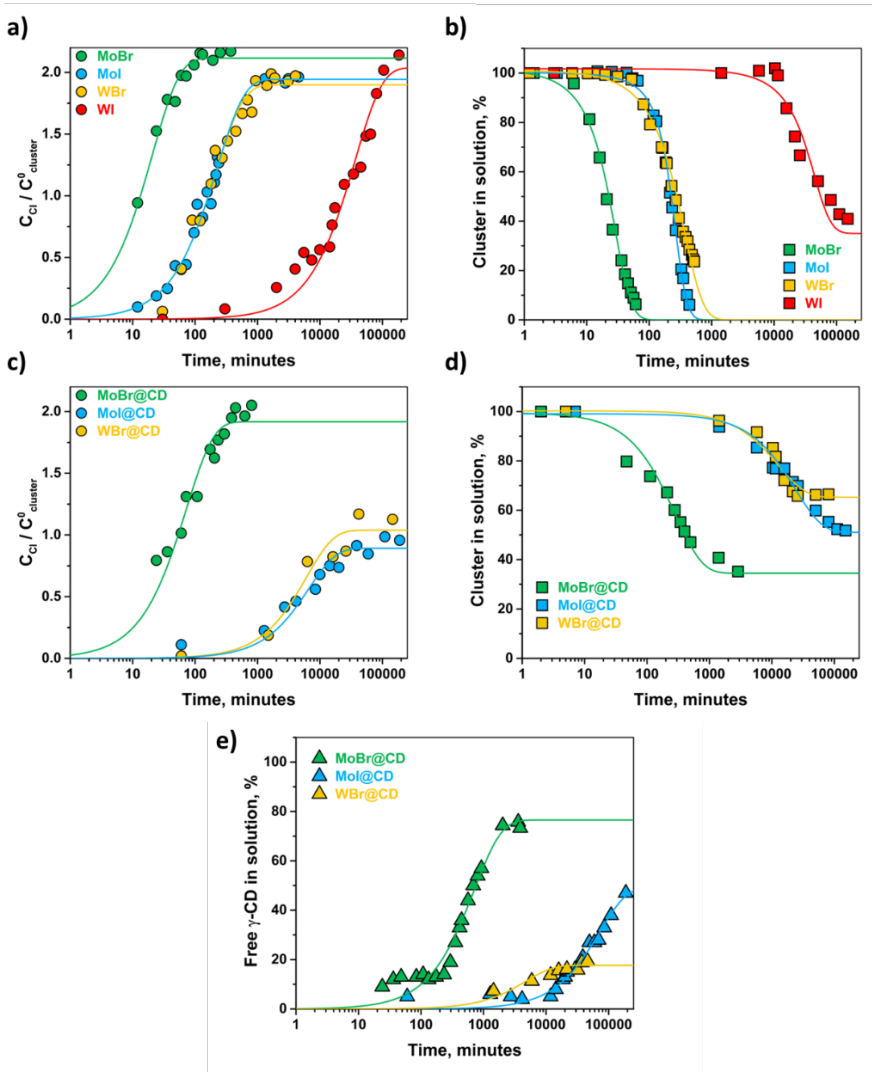

Figure 4. Monitoring of stability of $\{M_6X_8\}$ cluster with and without γ-CD in aqueous solution at room temperature (27 °C) by (a,b) ^{35}Cl NMR, (c,d) UV-vis and (e) ^{1}H NMR: (a,c) plot of Cl^- released in solution. The concentration of free chloride was quantified from integration of ^{35}Cl NMR signal using an external reference. (b,d) plots of UV-vis detected amount of cluster in solution of **MX@CD** and **MX**. The clusters content has been determined considering that $[\{M_6X_8\}Cl_6]^{2-}$ and $[\{M_6X_8\}(H_2O)Cl_5]^-$ exhibit similar absorption UV-vis spectra. (e) plot of CD release profile. The fraction of free CD generated after decomposition is determined from integrating signals of H1 (4.9-5.1 ppm range).

Despite the γ-CD significantly improved the stability of clusters in water, to different degrees depending on the system, precipitation of insoluble solids was still observed. For a more detailed study of the effect of cyclodextrin on the stabilization of clusters in aqueous solution, we have studied the kinetics of these processes by combining several methods. ^{35}Cl NMR is employed to measure the released chloride ligand in solution. Because of the spherical environment of aquo Cl^- anions with highly symmetric electric field gradient around ^{35}Cl, its detection by NMR becomes easy. To determine the concentration of the remaining solubilized clusters including those partially hydrolyzed, UV-vis spectroscopy is used. These measurements allow us to deduce the amount of precipitated $[\{M_6X_8\}(H_2O)_2Cl_4]$ cluster units. Finally, ^{1}H NMR allows to determine the released γ-CD upon hydrolysis of the clusters and decomplexation process. Figure 4 illustrates the summary of results as trends (considering pseudo first-order reaction models) of C_{Cl}, cluster or γ-CD content in solution for all systems *vs* time, while overall results are shown in the Supporting Information (Figures S5-S8).

Quantitative ^{35}Cl NMR investigation of initial clusters (in the absence of the CD) revealed that the hydrolysis process corresponds to the release of about 2 ± 0.25 Cl^- per cluster while the kinetics

depends strongly on the nature of the cluster core $\{M_6X_8\}$ (Table S2, Figure 4a). The rate of the hydrolysis process increases with the following order: $\{W_6I_8\} < \{W_6Br_8\} \approx \{Mo_6I_8\} < \{Mo_6Br_8\}$. The same trend is observed by UV-vis spectroscopy, showing that 50% of the cluster precipitated after 20 min, 3.5 h, 4 h and 43 days at room temperature (27 °C) for $\{Mo_6Br_8\}$, $\{Mo_6I_8\}$, $\{W_6Br_8\}$ and $\{W_6I_8\}$, respectively (Figure 4b). Noted that only in the case of **WI**, upon prolonged standing (more than 11 days), the spectrum profile begins to change, which may indicate the formation of more stable forms of clusters, possibly with a different ligand environment. This study shows that tungsten clusters are much more stable, at least from a kinetic point of view, than their equivalent molybdenum derivatives. This observation is not limited to clusters with terminal chloride ligands since a similar trend was also reported with terminal DMSO ligands.[28] Also, a higher stability of compounds with X = I than their bromide analogues was observed. This behavior appears to be related to the size of the inner ligands, which may also make the substitution of the apical ligands more difficult, probably by steric hindrance effect. On the other hand, the σ-donor character of the inner ligand is higher for $\{M_6Br_8\}$ than for $\{M_6I_8\}$. Therefore, the orbital overlap of the M-Cl σ bond is stronger for $\{M_6I_8\}$ cluster core, giving it greater stability for $[\{M_6I_8\}Cl_6]^{2-}$ clusters compared to $[\{M_6Br_8\}Cl_6]^{2-}$.

As for the native clusters, we studied stability of the compounds **MX@CD** in water over 3 months using ^{35}Cl and ^{1}H NMR, and UV-vis technique. According to ^{35}Cl NMR results, in all cases, a decrease of Cl^- release rate was observed when compared to the corresponding pristine cluster (Figure 4c). Remarkably, for **WI@CD**, no ^{35}Cl NMR signal corresponding to free Cl^- anions could be detected even after three months as well as unchangeable UV-vis spectrum was found (Figure S8d), indicating excellent host-guest stabilization. The cluster stability within the **MX@CD** adduct follows the trend observed in the **MX** series. Indeed, the less stable **MoBr@CD**

complex releases two Cl anions, while the other **MoI@CD** and **WBr@CD** release only one Cl anion, which indicates a difference in the affinity with CD. ^{1}H NMR investigation indicates the presence of free γ-CD after three months at different levels depending on the compound, ca. 20% for **WBr@CD,** 50% for **MoI@CD,** and 70% for **MoBr@CD** (Figure 4e). Such a difference in limit values of free CDs should account for the difference in affinity constants between the CD and a given cluster which requires different level of free CD to shift totally the equilibrium toward the **MX@CD** complex. This would happen as for the pristine cluster in two steps according to equations 3 and 4. The released CD will then shift progressively the equilibrium of adduct formation (equation 5) until stabilizing it definitively and no longer decomposition occurs at a given level of free CD which depends on the formation constant of the **MX@CD** complex. Furthermore, novel ^{1}H NMR signatures appeared in spectra of all these three compounds and increased with time, that are undoubtedly related to the inclusion of hydrolytic cluster products $[\{M_6X_8\}(H_2O)Cl_5]^-$ within the γ-CD cavity (see equations 3 and 4). Based on the chaotropic effect considerations, the $[\{M_6X_8\}(H_2O)Cl_5]^-$ entities are expected to exhibit increased affinity to the CD host due to its reduced charge density.[11, 12, 29] This fact can explain in part why the clusters containing $\{Mo_6I_8\}$ or $\{W_6Br_8\}$ core do not fully precipitate as revealed by UV-vis (Figure 4d).

$$[\{M_6X_8\}Cl_6@2\gamma\text{-CD}]^{2-} + H_2O \rightarrow [\{M_6X_8\}(H_2O)Cl_5@2\gamma\text{-CD}]^- + Cl^- \quad (3)$$

$$[\{M_6X_8\}(H_2O)Cl_5@2\gamma\text{-CD}]^- + H_2O \rightarrow [\{M_6X_8\}(H_2O)_2Cl_4]_{\downarrow} + 2\ \gamma\text{-CD} + Cl^- \quad (4)$$

$$[\{M_6X_8\}(H_2O)Cl_5]^- + 2\gamma\text{-CD} \rightleftarrows [\{M_6X_8\}(H_2O)Cl_5@2\gamma\text{-CD}]^- \quad (5)$$

We attempted to provide quantitative global analysis of the entire hydrolytic processes combining ^{35}Cl NMR, ^{1}H NMR and UV-vis spectroscopy and considering pseudo first-order reaction models (see Tables S1 and S2). From ^{35}Cl NMR data, kinetics of Cl^- release are obtained,

whereas ^{1}H NMR provides kinetics of CD release upon cluster decomposition. While ^{1}H NMR and UV-vis kinetics are comparable, ^{35}Cl NMR showed one order of magnitude faster processes that should indicate more complex reaction paths. This is fully consistent with the formation of new other complexes involving partially hydrolysed clusters as confirmed by the appearance of new ^{1}H NMR features. Therefore, the kinetics of clusters degradation probed by UV-vis and ^{1}H NMR are always slower than the Cl^- release. Addition of more γ-CD to the solutions will then shift the equilibriums to inclusion compounds $\{[\{M_6X_8\}Cl_6]@2\gamma\text{-CD}\}^{2-}$ and consequently increase the stability of the octahedral clusters. Also, the enrichment of the aqueous solution with NaCl will reduce the hydrolytic attack of water and will therefore also help to improve the stability of the **MX@CD** adducts. Thus, additional experiments have been carried out to verify such assumptions and the results are included in Figure S9. Three test tubes containing $[\{Mo_6I_8\}Cl_6]^{2-}$ and i) two equivalents of γ-CD in H_2O, ii) three equivalents of γ-CD in H_2O and iii) three equivalents of γ-CD in saline solution (0.9 wt.% NaCl) were left to stand for 42 days. Cluster concentrations were then measured using UV-vis spectroscopy, revealing 44% of the cluster was precipitated in the control first tube, against only 11% in the second one containing additional γ-CD, while almost no precipitation was observed in the third test tube. This clearly demonstrates the equilibrium displacement toward $[\{M_6X_8\}Cl_6]^{2-}$ and complexed forms upon increasing of Cl^- and γ-CD concentration in solution correspondingly.

In order to progress in the study of the biological properties of compounds, an important step is the transition from aqueous solutions to biological media. Another pH, the presence of different compounds and salts in solution, etc. (Table S4) can significantly affect the stability of clusters. Therefore, using UV-vis we also studied the behavior of the complexes and compounds with γ-CD (Figure S10-S12) in the culture medium (Dulbecco's Modified Eagle's Medium/Nutrient

Mixture F-12 Ham, Table S4) – commercial solution used for biological studies. According to the data obtained, the initial molybdenum clusters show similar hydrolysis curves at a slightly higher rate (Figure S11a,c). While the tungsten clusters showed a more specific behavior (Figure S11e,f) – the spectral profiles change with time (after 1 h or 12 days for **WBr** or **WI** correspondingly), which indicates either a significant modification of ligand environment or the complete destruction of the complexes, and therefore it is difficult to compare the data with those obtained in pure water. Moreover, it is observed that after a few days, all the clusters except **WI** hydrolyze completely, preventing the study of their biological properties. In the presence of γ-CD, the cluster complexes are also more stable, but the hydrolysis process is slightly different. While **MoBr@CD** (Figure S12a,b) and **WBr@CD** (Figure S12e,f) showed comparable kinetics to those occurring in pure water medium, 1.5 times faster process is observed for **MoI@CD** (Figure S12c,d). The amount of the remaining complexes in the solution is much less compared to the experiment in an aqueous solution (0, 22, and 52% in DMEM versus 38, 53, and 64% in pure water for **MoBr@CD**, **MoI@CD**, and **WBr@CD**, respectively). Only in the case of **WI@CD** (Figure S12g) the UV-vis spectrum did not change for at least a month, which confirms the exceptional stability of the complex in the culture medium as in pure water. It is also important to note that during three days (the incubation time in biological experiments) only **MoBr@CD** almost completely precipitate from the solution, while for **MoI@CD** and **WBr@CD** about 83 and 94% of cluster, respectively, remains in solution, which allow us to study the biological properties of compounds.

Luminescent properties of systems with γ-CD in solid state and aqueous solution

The supramolecular stabilization of $[\{M_6X_8\}Cl_6]^{2-}$ allows us to bring important insights about the luminescence properties which are highly relevant for future applications of such supramolecular adducts. Upon UV irradiation, inclusion compounds $Na_2[\{M_6X_8\}Cl_6@2\gamma\text{-CD}]$ and

$Na_2[\{M_6X_8\}Cl_6@2\gamma\text{-CD}]\cdot\gamma\text{-CD}$ exhibit typical for such clusters bright red/NIR emission in the solid-state and aqueous solutions (aerated and deaerated) with photophysical parameters presented in Table 1 (further details can be found in the Supporting Information, see Figures S13-S38 and Table S2). Despite the shielding effect of γ-CD for $[\{M_6X_8\}Cl_6]^{2-}$ significant decrease of the luminescence lifetimes and quantum yields in aerated conditions was observed almost in all cases. This evidences the cluster triplet-excited state quenching by molecular oxygen, with the formation of singlet oxygen species $^1O_2$. The direct measurements of the singlet oxygen phosphorescence at about 1270 nm in D_2O did confirm $^1O_2$ formation (Figures S39-S40, in the Supporting Information).

Table 1. Main photophysical characteristics of $Na_2\{[\{M_6X_8\}Cl_6]@2\gamma\text{-CD}\}\cdot nH_2O$ (**MX@CD**) (M = Mo, W; X = Br, I) in the solid state and in water solution. λ – maxima of the luminescence bands, τ – emission lifetimes, τ_0 – amplitude average emission lifetimes and Φ – the luminescence quantum yield.

Compound	MoBr@CD	MoI@CD	WBr@CD	WI@CD
Solid state				
λ, nm	725	690[a]	755	665
τ (A), μs	94.5 (54%) 35.6 (46%)	133[a]	22.2 (1%) 5.4 (9%) 1.5 (90%)	16.2 (51%) 7.4 (49%)
τ_0, μs	67.4	133[a]	2.1	11.9
Φ	0.07	0.40[a]	0.03	0.26
Aerated water solution				
λ, nm	710	690	730	665

τ (A), μs	37.5 (69%) 16.6 (31%)	42.8	8.4 (6%) 2.0 (94%)	4.9
τ_0, μs	31.0	42.8	2.4	4.9
Φ	0.04	0.08	0.02	0.08
Deaerated water solution				
τ (A), μs	91.0 (70%) 21.3 (30%)	119	14.4 (8%) 2.0 (92%)	15.3 (75%) 7.2 (25%)
τ_0, μs	70.1	119	3.0	13.3
Φ	0.05	0.16	0.01	0.11

[a] data from ref. [20]

Biological properties of supramolecular compounds

All results described above demonstrated clearly that γ-cyclodextrin strongly stabilizes octahedral halide clusters in aqueous solutions, and the resulting inclusion compounds exhibit bright red/NIR emission. All these promising results motivate us to investigate the biological properties. We evaluated i) dark and photo-induced cytotoxicity and ii) cellular uptake on HeLa (cervical epithelioid carcinoma) and NAF2nor (immortalized human fibroblasts) cell lines.

Mostly, according to MTT-assay (Figure 5a,b) in the studied concentration range (2-1250 μM), IC_{50} values are more than 600 μM (Table S6) indicating moderate cytotoxicity. In the case of the least stable complex **MoBr@CD**, an increase in cell viability (>100%) is observed, which rather indicates the destruction and precipitation of the complex (which is consistent with the stability results described above) and the release of γ-cyclodextrin in the solution. This fact is confirmed by the data of confocal microscopy: only in the case of **MoBr@CD**, the formation of precipitates (Figure S43 and S44) is observed which are "sticked" or entered the cells (Figure S43-S45). Also, according to microscopy, there is no penetration of tungsten clusters into cells (Figure S43 and

S44) and minimal penetration in the case of **MoBr@CD** (Figure S45). Such observations are also supported by flow cytometry (FACS) data (Figures 5c, S41 and S42). Mo_6-clusters were uptaken noticeably better by HeLa cells than tungsten one. One can see, that according to FACS data compounds didn't penetrate to the healthy cells (Figure 5c). However, given the more intense autofluorescence of healthy cells compared to cancer cells (intensity $\backsim 2 \cdot 10^5$ versus $8 \cdot 10^4$), it was more difficult to detect the luminescence of compounds. Additionally, photo-induced cytotoxicity was evaluated at a non-toxic concentration (31.25-125 μM) of **MX@CD** under light-irradiation ($\lambda \geq 400$ nm) for 30 minutes. In general, the compounds exhibit no phototoxicity (Figures S46-S47, in the Supporting Information), which probably is related to the shielding effect of γ-CD. Based on the obtained results (low toxicity, low penetration and absence of phototoxicity), one can assume the use of such host-guest complexes as carriers of cluster compounds (release and penetration into cells during hydrolysis) or as radiopaque agents, since molybdenum and tungsten clusters, due to heavy elements in the cluster core, exhibit high contrast properties.[30, 31]

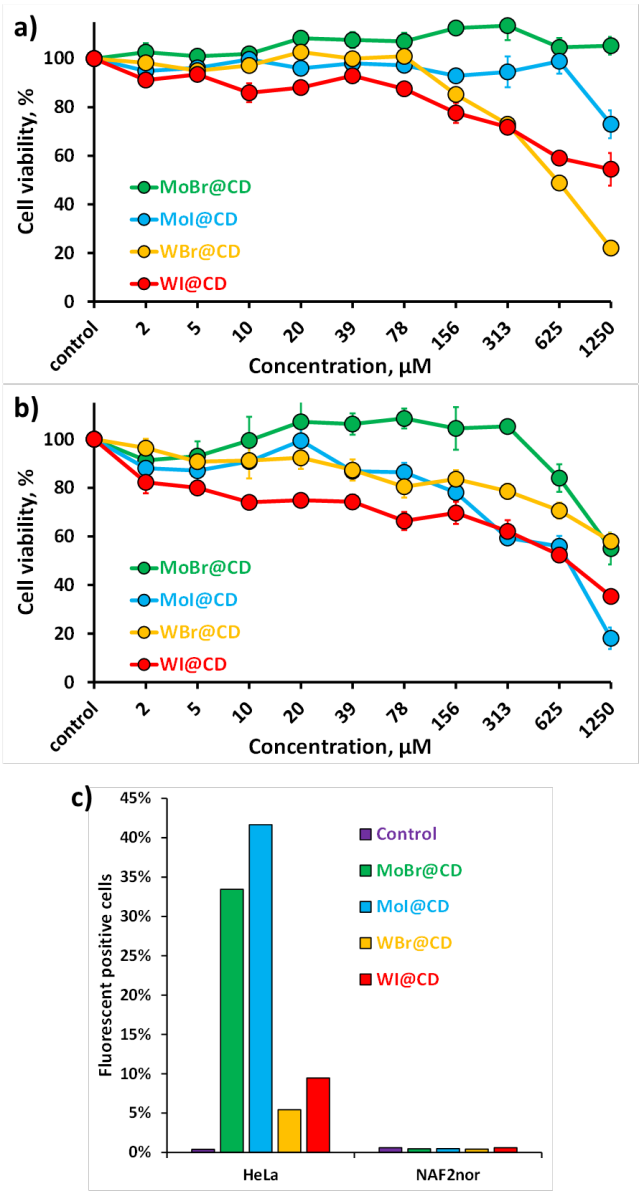

Figure 5. The effect of inclusion compounds $Na_2[\{M_6X_8\}Cl_6@2\gamma\text{-CD}]\cdot nH_2O$ (**MX@CD**) on HeLa (a) and NAF2nor (b) cell viability, and comparison of cellular uptake of clusters by different cell lines according to FACS (c).

Conclusions

We demonstrate that γ-CD interacts with Mo and W octahedral-type clusters $[\{M_6X_8\}Cl_6]^{2-}$ to form highly stable inclusion complexes, offering a protecting shell to avoid the chlorine substitution by

water molecules, and consequently improving drastically their stability in aqueous solution. Furthermore, the resulting composite adducts had led to a bright luminescence due to the shielding effect of γ-CD. Such shielding effect of this natural benign macrocyclic molecule contributes further in minimizing the phototoxicity of the inorganic cluster. The low dark and photo-induced cytotoxicity of the inclusion compounds open new horizons in the field of biomedical applications such as X-ray contrast imaging or drug delivery.

ASSOCIATED CONTENT

Supporting Information.

The Supporting Information is available free of charge on the ACS Publications website at DOI:
The following files are available free of charge.
Single crystal XRD data; NMR measurements; UV-vis spectroscopy data; Luminescence data; Confocal microscopy and FACS data.

AUTHOR INFORMATION

Corresponding Authors

Anton A. Ivanov - *Nikolaev Institute of Inorganic Chemistry SB RAS, 3 Acad. Lavrentiev Ave., 630090 Novosibirsk, Russian Federation*

orcid.org/0000-0003-2026-8568

e-mail: ivanov338@niic.nsc.ru

Mohamed Haouas - *Institut Lavoisier de Versailles, UMR 8180 CNRS, UVSQ, Université Paris-Saclay, Versailles, France.*

orcid.org/ 0000-0002-2133-702X

e-mail: mohamed.haouas@uvsq.fr

Michael A. Shestopalov – *Nikolaev Institute of Inorganic Chemistry SB RAS, 3 Acad. Lavrentiev Ave., 630090 Novosibirsk, Russian Federation*

orcid.org/0000-0001-9833-6060

e-mail: shtopy@niic.nsc.ru

Authors

Darya V. Evtushok – *Nikolaev Institute of Inorganic Chemistry SB RAS, 3 Acad. Lavrentiev Ave., 630090 Novosibirsk, Russian Federation*

orcid.org/0000-0003-0508-6117

Tatiana N. Pozmogova – *Nikolaev Institute of Inorganic Chemistry SB RAS, 3 Acad. Lavrentiev Ave., 630090 Novosibirsk, Russian Federation*

orcid.org/0000-0002-7399-0530

Tatiana S. Golubeva – *Federal Research Center Institute of Cytology and Genetics SB RAS, Novosibirsk, Russia.*

orcid.org/0000-0002-4400-0665

Yann Molard – *Université de Rennes, CNRS, ISCR - UMR 6226, ScanMAT – UMS 2001, F-35000 Rennes.*

orcid.org/0000-0002-6295-0883

Stéphane Cordier – *Université de Rennes, CNRS, ISCR - UMR 6226, ScanMAT – UMS 2001, F-35000 Rennes.*

orcid.org/0000-0003-0707-3774

Clément Falaise – *Institut Lavoisier de Versailles, UMR 8180 CNRS, UVSQ, Université Paris-Saclay, Versailles, France*.

orcid.org/0000-0003-2000-3113

Emmanuel Cadot – *Institut Lavoisier de Versailles, UMR 8180 CNRS, UVSQ, Université Paris-Saclay, Versailles, France*.

orcid.org/0000-0003-4136-6298

Author Contributions

The manuscript was written through contributions of all authors. All authors have given approval to the final version of the manuscript.

Funding Sources

The Grant of the President of the Russian Federation (grant no. МД-123.2022.1.3)

Ministry of Science and Higher Education of the Russian Federation (№ 121031700321-3)

Labex charmmmat, ANR-11-LBX-0039-grant

Notes

The authors declare no competing financial interest.

ACKNOWLEDGMENT

The Authors gratefully acknowledge financial support from LIA-CNRS CLUSPOM. NIIC team thanks the Grant of the President of the Russian Federation (grant № МД-123.2022.1.3) and the Ministry of Science and Higher Education of the Russian Federation (№ 121031700321-3). This

work was also supported by public grants overseen by i) University of Versailles Saint Quentin, ii) CNRS, iii) Region Île-de-France, iv) and French National Research Agency (ANR) as part of the "Investissements d'Avenir" program (Labex charmmmat, ANR-11-LBX-0039-grant). The authors thank the Collective Center of ICG SB RAS "Collection of Pluripotent Human and Mammalian Cell Cultures for Biological and Biomedical Research" (http://ckp.icgen.ru/cells/; http://www.biores.cytogen.ru/brc_cells/collections/ICG_SB_RAS_CELL) for providing the NAF2nor cell lines and Center for Collective Use of Microscopic Analysis of Biological Objects ICG SB RAS for providing the equipment for confocal microscopy. AAI is grateful to Embassy of France in Russian Federation for Vernadsky scholarship for post-graduate students.

REFERENCES

1. Davis, M. E.; Brewster, M. E. Cyclodextrin-based pharmaceutics: past, present and future. *Nat. Rev. Drug Discov.* **2004,** 3, 1023-1035 DOI: 10.1038/nrd1576.

2. Assaf, K. I.; Ural, M. S.; Pan, F.; Georgiev, T.; Simova, S.; Rissanen, K.; Gabel, D.; Nau, W. M. Water structure recovery in chaotropic anion eecognition: high-affinity binding of dodecaborate clusters to γ-cyclodextrin. *Angew. Chem. Int. Ed.* **2015,** 54 (23), 6852-6856 DOI: 10.1002/anie.201412485.

3. Ivanov, A. A.; Falaise, C.; Abramov, P. A.; Shestopalov, M. A.; Kirakci, K.; Lang, K.; Moussawi, M. A.; Sokolov, M. N.; Naumov, N. G.; Floquet, S.; Landy, D.; Haouas, M.; Brylev, K. A.; Mironov, Y. V.; Molard, Y.; Cordier, S.; Cadot, E. Host–guest binding hierarchy within redox- and luminescence-responsive supramolecular self-assembly based on chalcogenide clusters and γ-cyclodextrin. *Chem. Eur. J.* **2018,** 24 (51), 13467-13478 DOI: 10.1002/chem.201802102.

4. Moussawi, M. A.; Leclerc-Laronze, N.; Floquet, S.; Abramov, P. A.; Sokolov, M. N.; Cordier, S.; Ponchel, A.; Monflier, E.; Bricout, H.; Landy, D.; Haouas, M.; Marrot, J.; Cadot, E. Polyoxometalate, cationic cluster, and γ-cyclodextrin: from primary interactions to supramolecular hybrid materials. *J. Am. Chem. Soc.* **2017,** 139 (36), 12793-12803 DOI: 10.1021/jacs.7b07317.

5. Moussawi, M. A.; Haouas, M.; Floquet, S.; Shepard, W. E.; Abramov, P. A.; Sokolov, M. N.; Fedin, V. P.; Cordier, S.; Ponchel, A.; Monflier, E.; Marrot, J.; Cadot, E. Nonconventional three-component hierarchical host–guest assembly based on Mo-blue ring-shaped giant anion, γ-cyclodextrin, and Dawson-type polyoxometalate. *J. Am. Chem. Soc.* **2017,** 139 (41), 14376-14379 DOI: 10.1021/jacs.7b08058.

6. Wu, Y.; Shi, R.; Wu, Y.-L.; Holcroft, J. M.; Liu, Z.; Frasconi, M.; Wasielewski, M. R.; Li, H.; Stoddart, J. F. Complexation of polyoxometalates with cyclodextrins. *J. Am. Chem. Soc.* **2015,** 137 (12), 4111-4118 DOI: 10.1021/ja511713c.

7. Falaise, C.; Moussawi, M. A.; Floquet, S.; Abramov, P. A.; Sokolov, M. N.; Haouas, M.; Cadot, E. Probing dynamic library of metal-oxo building blocks with γ-cyclodextrin. *J. Am. Chem. Soc.* **2019,** 140 (36), 11198 DOI: 10.1021/jacs.8b07525.

8. Singleton, M. L.; Crouthers, D. J.; Duttweiler, R. P.; Reibenspies, J. H.; Darensbourg, M. Y. Sulfonated diiron complexes as water-soluble models of the [Fe–Fe]-hydrogenase enzyme active site. *Inorg. Chem.* **2011,** 50 (11), 2015-5026 DOI: 10.1021/ic200272x.

9. Singleton, M. L.; Reibenspies, J. H.; Darensbourg, M. Y. A cyclodextrin host/guest approach to a hydrogenase active site biomimetic cavity. *J. Am. Chem. Soc.* **2010,** 132 (26), 8870–8871 DOI: 10.1021/ja103774j.

10. Yao, S.; Falaise, C.; Leclerc, N.; Roch-Marchal, C.; Haouas, M.; Cadot, E. Improvement of the hydrolytic stability of the Keggin molybdo- and tungsto-phosphate anions by cyclodextrins. *Inorg. Chem.* **2022,** 61 (9), 4193–4203 DOI: 10.1021/acs.inorgchem.2c00095.

11. Assaf, K. I.; Nau, W. M. The chaotropic effect as an assembly motif in chemistry. *Angew. Chem. Int. Ed.* **2018,** 57 (43), 13968-13981 DOI: 10.1002/anie.201804597.

12. Ivanov, A. A.; Falaise, C.; Landy, D.; Haouas, M.; Mironov, Y. V.; Shestopalov, M. A.; Cadot, E. Tuning the chaotropic effect as an assembly motif through one-electron transfer in a rhenium cluster. *Chem. Commun.* **2019,** 55 (67), 9951-9954 DOI: 10.1039/C9CC05136H.

13. Kirakci, K.; Kubát, P.; Fejfarová, K.; Martinčík, J.; Nikl, M.; Lang, K. X-ray inducible luminescence and singlet oxygen sensitization by an octahedral molybdenum cluster compound: a new class of nanoscintillators. *Inorg. Chem.* **2016,** 55 (2), 803-809 DOI: 10.1021/acs.inorgchem.5b02282.

14. Maverick, A. W.; Najdzionek, J. S.; MacKenzie, D.; Nocera, D. G.; Gray, H. B. Spectroscopic, electrochemical, and photochemical properties of molybdenum(II) and tungsten(II) halide clusters. *J. Am. Chem. Soc.* **1983,** 105 (7), 1878-1882 DOI: 10.1021/ja00345a034.

15. Nocera, D. G.; Gray, H. B. Electrochemical reduction of molybdenum(II) and tungsten(II) halide cluster ions. Electrogenerated chemiluminescence of tetradecachlorohexamolybdate(2-) ion. *J. Am. Chem. Soc.* **1984,** 106 (3), 824-825 DOI: 10.1021/ja00315a079.

16. Kirakci, K.; Pozmogova, T. N.; Protasevich, A. Y.; Vavilov, G. D.; Stass, D. V.; Shestopalov, M. A.; Lang, K. A water-soluble octahedral molybdenum cluster complex as a

potential agent for X-ray induced photodynamic therapy. *Biomater. Sci.* **2021,** 9 (8), 2893-2902 DOI: 10.1039/D0BM02005B.

17. Solovieva, A. O.; Vorotnikov, Y. A.; Trifonova, K. E.; Efremova, O. A.; Krasilnikova, A. A.; Brylev, K. A.; Vorontsova, E. V.; Avrorov, P. A.; Shestopalova, L. V.; Poveshchenko, A. F.; Mironov, Y. V.; Shestopalov, M. A. Cellular internalisation, bioimaging and dark and photodynamic cytotoxicity of silica nanoparticles doped by $\{Mo_6I_8\}^{4+}$ metal clusters. *J. Mater. Chem. B* **2016,** 4 (28), 4839-4846 DOI: 10.1039/C6TB00723F.

18. Svezhentseva, E. V.; Solovieva, A. O.; Vorotnikov, Y. A.; Kurskaya, O. G.; Brylev, K. A.; Tsygankova, A. R.; Edeleva, M. V.; Gyrylova, S. N.; Kitamura, N.; Efremova, O. A.; Shestopalov, M. A.; Mironov, Y. V.; Shestopalov, A. M. Water-soluble hybrid materials based on $\{Mo_6X_8\}^{4+}$ (X = Cl, Br, I) cluster complexes and sodium polystyrene sulfonate. *New J. Chem.* **2017,** 41 (4), 1670-1676 DOI: 10.1039/C6NJ03469A.

19. Felip-León, C.; Valle, C. A. d.; Pérez-Laguna, V.; Millán-Lou, M. I.; Miravet, J. F.; Mikhailov, M.; Sokolov, M. N.; Rezusta-López, A.; Galindo, F. Superior performance of macroporous over gel type polystyrene as a support for the development of photo-bactericidal materials. *J. Mater. Chem. B* **2017,** 5 (30), 6058-6064 DOI: 10.1039/C7TB01478C.

20. Falaise, C.; Ivanov, A. A.; Molard, Y.; Amela Cortes, M.; Shestopalov, M. A.; Haouas, M.; Cadot, E.; Cordier, S. From supramolecular to solid state chemistry: crystal engineering of luminescent materials by trapping molecular clusters in an aluminium-based hosting matrix. *Mater. Horiz.* **2020,** 7 (9), 2399-2406 DOI: 10.1039/D0MH00637H.

21. Hogue, R. D.; McCarley, R. E. Chemistry of polynuclear metal halides. V. reactions and characterization of compounds containing tungsten halide cluster species. *Inorg. Chem.* **1970,** 9 (6), 1354-1360 DOI: 10.1021/ic50088a012.

22. Dolomanov, O. V.; Bourhis, L. J.; Gildea, R. J.; Howard, J. a. K.; Puschmann, H. OLEX2: a complete structure solution, refinement and analysis program. *J. Appl. Cryst.* **2009,** 42 (2), 339-341 DOI: 10.1107/S0021889808042726.

23. Sheldrick, G. M. SHELXT – Integrated space-group and crystal-structure determination. *Acta Cryst. A* **2015,** 71 (1), 3-8 DOI: 10.1107/S2053273314026370.

24. Sheldrick, G. M. Crystal structure refinement with SHELXL. *Acta Cryst. C* **2015,** 71 (1), 3-8 DOI: 10.1107/S2053229614024218.

25. Savitzky, A.; Golay, M. J. E. Smoothing and differentiation of data by simplified least squares procedures. *Anal. Chem.* **1964,** 36 (8), 1627–1639 DOI: 10.1021/ac60214a047.

26. Guggenberger, L. J.; Sleight, A. W. Structural and bonding characterizations of molybdenum dibromide, $Mo_6Br_{12}.2H_2O$. *Inorg. Chem.* **1969,** 8 (10), 2041-2049 DOI: 10.1021/ic50080a001.

27. Schäfer, H.; Plautz, H. Die dihydrate $[Me_6X_8]X_4 \cdot 2H_2O$ mit Me = Mo, W; X = Cl, Br, I. *Z. Anorg. Allg. Chem.* **1972,** 389 (1), 57-67 DOI: 10.1002/zaac.19723890107.

28. Svezhentseva, E. V.; Vorotnikov, Y. A.; Solovieva, A. O.; Pozmogova, T. N.; Eltsov, I. V.; Ivanov, A. A.; Evtushok, D. V.; Miroshnichenko, S. M.; Yanshole, V. V.; Eling, C. J.; Adawi, A. M.; Bouillard, J.-S. G.; Kuratieva, N. V.; Fufaeva, M. S.; Shestopalova, L. V.; Mironov, Y. V.; Efremova, O. A.; Shestopalov, M. A. From photoinduced to dark cytotoxicity through an

octahedral cluster hydrolysis. *Chem. Eur. J.* **2018,** 24 (68), 17915-17920 DOI: 10.1002/chem.201804663.

29. Yao, S.; Falaise, C.; Ivanov, A. A.; Leclerc, N.; Hohenschutz, M.; Haouas, M.; Landy, D.; Shestopalov, M. A.; Bauduin, P.; Cadot, E. Hofmeister effect in the Keggin-type polyoxotungstate series. *Inorg. Chem. Front.* **2021,** 8 (1), 12-25 DOI: 10.1039/D0QI00902D.

30. Evtushok, D. V.; Melnikov, A. R.; Vorotnikova, N. A.; Vorotnikov, Y. A.; Ryadun, A. A.; Kuratieva, N. V.; Kozyr, K. V.; Obedinskaya, N. R.; Kretov, E. I.; Novozhilov, I. N.; Mironov, Y. V.; Stass, D. V.; Efremova, O. A.; Shestopalov, M. A. A comparative study of optical properties and X-ray induced luminescence of octahedral molybdenum and tungsten cluster complexes. *Dalton Trans.* **2017,** 46 (35), 11738-11747 DOI: 10.1039/C7DT01919J.

31. Krasilnikova, A. A.; Shestopalov, M. A.; Brylev, K. A.; Kirilova, I. A.; Khripko, O. P.; Zubareva, K. E.; Khripko, Y. I.; Podorognaya, V. T.; Shestopalova, L. V.; Fedorov, V. E.; Mironov, Y. V. Prospects of molybdenum and rhenium octahedral cluster complexes as X-ray contrast agents. *J. Inorg. Biochem.* **2015,** 144, 13-17 DOI: 10.1016/j.jinorgbio.2014.12.016.

For Table of Contents Only

γ-cyclodextrin drastically increases the stability of molybdenum and tungsten octahedral clusters in water offering new perspectives for their use in biomedicine